Quantum state transfer through disordered hexagonal lattices

D. Messias,[1] C. V. C. Mendes,[1] R. F. Dutra,[1] G. M. A. Almeida,[1] M. L. Lyra,[1] and F. A. B. F. de Moura[1,*]

[1] *Instituto de Física, Universidade Federal de Alagoas, 57072-900 Maceió, AL, Brazil*

(Dated: March 16, 2023)

We investigate a quantum-state transfer protocol through a quasi-1D spin-1/2 channel defined on a hexagonal layer featuring hopping disorder. In the absence of disorder, the quantum channel display two flat bands hosting compact localized states. That is signalled by the appearance of singularities in the density of states. We show that an arbitrary qubit state can be transmitted with high fidelity between the two ends even in the presence of noise as long as they are not in resonance with energy levels surrounding the flat band. This higher sensitivity against disorder is due to the residual single-cell compact localized states accompanied by a degeneracy lifting.

I. INTRODUCTION

Quantum information technologies have gone through significant advances in recent years. Although all-round commercial quantum computing is still far from reality, big tech companies are making progress with superconducting-based quantum computers featuring tens of qubits [1, 2]. Yet, there is plenty of room for improvement, specially when it comes to fault-tolerant quantum computing. As put by Preskill in [3], we are currently in the era noisy intermediate-scale quantum devices, meaning that although computers featuring tens of qubits are already available, they face limitations on their performance due to imperfect control over qubits and quantum gates. It is thus paramount to find out ways to deal with noise so as to develop more accurate quantum processing units.

Large-scale quantum information processing demands robust quantum-state transfer (QST) and entanglement generation protocols between distant nodes in a network [4]. One approach consists of engineered solid-state qubit networks, carefully crafted to bypass active control as much as possible. A paradigmatic QST model was put forward by Bose in [5] on the framework of spin chains with nearest-neighbor exchange interaction acting as channels set to work via the natural time evolution of the system. Numerous works followed up addressing unique interaction patterns and topologies, each featuring different requirements, speed-fidelity tradeoffs, and so forth [6–24] (see Refs. [25, 26] for reviews). One of the issues underlying those engineered networks is the unavoidable presence of disorder due to parameter fluctuations that might occur during their fabrication/assembling process. The occurrence of Anderson localization phenomena in QST protocols has been explored in different settings [27–34]. QST protocols operating in the Rabi regime, that is when the sender and receiver are weakly coupled to the channel, are particularly robust against static disorder [28]. This trait has been explored considering various types of diagonal and off-diagonal disorder [33–35].

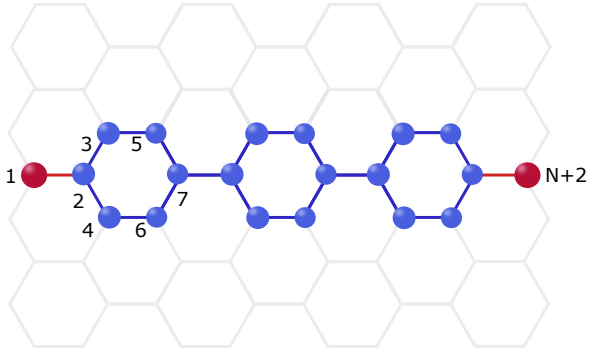

FIG. 1. QST model. A quasi-1D array defined on a hexagonal layer featuring hopping disorder constitutes the channel and the two outermost sites, weakly coupled to it, act as sender and receiver.

In this work, we go beyond 1D configurations and investigate the resilience of an isotropic XY spin-1/2 chain defined on honeycomb layers (see Fig. 1) featuring static interaction (off-diagonal) disorder. The aim is to look for novel topological features that can handle high-quality and robust QST. Indeed, polymer-based geometries provides rich spectral properties [36–39]. Lattices hosting flat bands – dispersionless bands associated to diverging density of states – are an example that has been largely explored in recent years [38–40]. The hexagonal strip of Fig. 1 hosts two flat bands each being populated by one-cell compact localized states.

We show that it is possible to perform end-to-end QST through the disordered lattice provided they are in close resonance with delocalized channel modes. In our case, that strictly means the flat-band levels must be avoided due to compact localized modes. This is explained in terms of the key spectral properties of the channel such as the density of states and participation ratio.

II. MODEL

Let us consider an isotropic XY spin-1/2 chain with N sites, arranged as a quasi-1D hexagonal array as shown in Fig. 1. The Hamiltonian of this system is written as

* fidelis@fis.ufal.br

$H = H_{ch} + H_I$, where

$$H_{ch} = \sum_{i=2}^{N+1} \frac{\epsilon_i}{2}(1-\hat{\sigma}_i^z) + \sum_{\langle i,j\rangle} \frac{J_{i,j}}{2}(\hat{\sigma}_i^x\hat{\sigma}_j^x + \hat{\sigma}_i^y\hat{\sigma}_j^y), \quad (1)$$

$$H_I = \frac{w}{2}(1-\hat{\sigma}_1^z) + \frac{g}{2}(\hat{\sigma}_1^x\hat{\sigma}_2^x + \hat{\sigma}_1^y\hat{\sigma}_2^y) + \frac{w}{2}(1-\hat{\sigma}_{N+2}^z) + \frac{g}{2}(\hat{\sigma}_{N+1}^x\hat{\sigma}_{N+2}^x + \hat{\sigma}_{N+1}^y\hat{\sigma}_{N+2}^y), \quad (2)$$

with $\hat{\sigma}_i^{x,y,z}$ denoting the Pauli operators acting on spin i, ϵ_i the local magnetic field (on-site energy), and J_{ij} the nearest-neighbor coupling strength between spins i and j. The sender (s) and receiver (r) spins residing on the end points couple to the channel via g and their local energies are both set to w.

It is immediate to see that the Hamiltonian preserves the total magnetization of the system, i.e., $[H, \sum_i \sigma_i^z] = 0$, so that it can be partitioned into subspaces with fixed excitation number. Here we will be concerned with the single-excitation subspace only for the following reason. To transfer an arbitrary qubit state [5] we may initialize the first spin (residing at the leftmost end) in $|\psi\rangle_1 = \alpha|\downarrow_1\rangle + \beta|\uparrow_1\rangle$, with the rest of the system in the ground state so that the whole system reads $|\Psi(0)\rangle = |\psi\rangle_1|\downarrow_2\cdots\downarrow_{N+1}\rangle|\downarrow_{N+2}\rangle$. Then, we let it evolve through the time evolution operator, $|\Psi(t)\rangle = e^{-iHt}|\Psi(0)\rangle$, what renders the actual dynamics to take place in the $(N+2)$-dimensional single-excitation subspace. So hereafter we set, for easiness, $|i\rangle \equiv |\downarrow_1\downarrow_2\cdots\uparrow_i\cdots\downarrow_{N+2}\rangle$. The goal of the protocol is to obtain, at some instant τ, the state $|\Psi(\tau)\rangle = |\downarrow_1\rangle|\downarrow_2\cdots\downarrow_{N+1}\rangle|\psi\rangle_{N+2}$ (not considering the global phase), which is when the qubit state has reached the rightmost end of the array.

To evaluate the transfer performance, the fidelity for a specific input reads $F_\psi = \langle\psi|\rho_{N+2}|\psi\rangle$, with $\rho_{N+2} = \mathrm{Tr}_{1,\ldots,N+1}|\Psi(\tau)\rangle\langle\Psi(\tau)|$. In order to obtain a measure that does not depend on amplitudes α and β, we can perform an average over the Bloch sphere to obtain [5]

$$F(t) = \frac{1}{2} + \frac{f_{N+2}(t)}{3}\cos\zeta + \frac{f_{N+2}(t)^2}{6}, \quad (3)$$

where $f_{N+2}(t) = |\langle N+2|e^{-iHt}|1\rangle|$ and $\cos\zeta \equiv 1$ by a convenient local rotation. Equation (3) falls within interval $[0.5, 1]$ reaching its maximum only when $f_{N+2} = 1$.

Let us now set all the on-site energies of the channel to $\epsilon_i = 0$ and rewrite the Hamiltonian in a much simpler form (in the single-excitation basis) as

$$H = \sum_{\langle i,j\rangle} J_{i,j}|i\rangle\langle j| + g(|1\rangle\langle 2| + |N+1\rangle\langle N+2|) + w(|1\rangle\langle 1| + |N+2\rangle\langle N+2|) + \text{h.c.}. \quad (4)$$

We further assume that the hopping strength $J_{i,j}$ is subjected to static noise of the form $J_{i,j}/J = 1 + \xi_{i,j}$, where $\xi_{i,j}$ is a random number falling in a box distribution $[-b, b]$, b denoting the disorder strength. Hereafter we set the energy units such that $J \equiv 1$.

Note that if $g \approx J$ an initial excitation will either get delocalized within the channel or undergo Anderson localization due to disorder. It is therefore not well suited for high-fidelity QST, especially between long distances. A way around is to set $g \ll J$ in order to energetically detach the communicating parties from the channel. Indeed, as put forward in [11], second-order perturbation theory in g yields the effective Hamiltonian spanned by $\{|1\rangle, |N+2\rangle\}$:

$$H_{\text{eff}} = \begin{pmatrix} h_s & J_{\text{eff}} \\ J_{\text{eff}} & h_r \end{pmatrix}, \quad (5)$$

where

$$h_\nu = w - g^2\sum_k \frac{|v_{\nu,k}|^2}{E_k - w}, \quad (6)$$

$$J_{\text{eff}} = -g^2\sum_k \frac{v_{s,k}v_{r,k}^*}{E_k - w}, \quad (7)$$

with $\nu \in \{s, r\}$, $v_{s,k} = \langle 2|E_k\rangle$, $v_{r,k} = \langle N+1|E_k\rangle$ and E_k, $|E_k\rangle$ being the eigenvalues and eigenvectors of H_{ch} respectively. Note that the off-resonant condition $E_k \neq w\ \forall\ k$ must hold for the equations above to be valid unless $v_{\nu,k} = 0$.

The weak-coupling regime approximately reduces the dynamics of the entire array to that of a two-level system involving the two outermost parties. However, the effective coupling and on-site energies carries information about the channel, being pivotal that $(h_s - h_r)/J_{\text{eff}}$ gets as close to zero as possible, or else we will get something that looks like a detuned two-level dynamics and hence poor transfer fidelity. In the ideal scenario $h_s - h_r = 0$ and the QST is reached at times $\tau = n\pi/(2|J_{\text{eff}}|)$, where $J_{\text{eff}} \propto g^2$.

Now, before evaluating the QST performance, let us gain some insight about how the channel modes will play out with the effective description above.

III. RESULTS

A. Spectral properties of the hexagonal lattice

In the absence of disorder, the density of states, $DOS(E) = \sum_k \delta(E - E_k)$, of the channel described by H_{ch} [Eq. (1)] can be treated analytically by mapping it onto an effective linear chain with alternate hoppings. Using a standard decimation procedure, the degrees of freedom corresponding to the internal sites of each cell can be eliminated, leading to an effective energy-dependent hopping amplitude between the connecting sites of a cell with renormalized energy-dependent on-site energies. Let us illustrate this decimation procedure

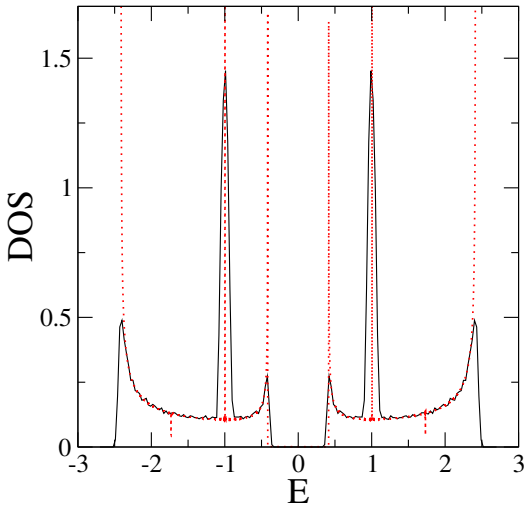

FIG. 2. Comparison between the analytic DOS obtained via the effective model derived for the ordered channel (dotted red line) and the DOS evaluated numerically for $b = 0.1J$ and $N = 600$ (solid black line).

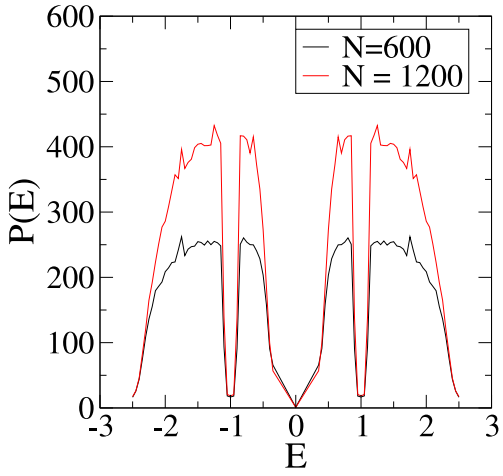

FIG. 3. Participation number for $N = 600, 1200$ and disorder strength $b = 0.1J$.

for a single arbitrary cell l using the site index adopted in Fig.1. Assuming $v_i^{(l)}$ as the eigenfuction amplitude at site i at the $l-th$ cell with corresponding eigenvalue E, we obtain the following set of coupled equations:

$$\begin{aligned}
Ev_2^{(l)} &= Jv_7^{(l-1)} + Jv_3^{(l)} + Jv_4^{(l)},\\
Ev_3^{(l)} &= Jv_2^{(l)} + Jv_5^{(l)},\\
Ev_4^{(l)} &= Jv_2^{(l)} + Jv_6^{(l)},\\
Ev_5^{(l)} &= Jv_3^{(l)} + Jv_7^{(l)},\\
Ev_6^{(l)} &= Jv_4^{(l)} + Jv_7^{(l)}\\
Ev_7^{(l)} &= Jv_5^{(l)} + Jv_6^{(l)} + Jv_2^{(l+1)}.
\end{aligned} \tag{8}$$

The amplitudes $v_3^{(l)}$, $v_4^{(l)}$, $v_5^{(l)}$ and $v_6^{(l)}$ can be eliminated from the above set, leading to effective equations for the connecting sites, namely

$$\begin{aligned}
Ev_2^{(l)} &= Jv_7^{(l-1)} + E_{eff}v_2^{(l)} + J_{eff}v_7^{(l)},\\
Ev_7^{(l)} &= E_{eff}v_7^{(l)} + J_{eff}v_2^{(l)} + Jv_2^{(l+1)},
\end{aligned} \tag{9}$$

with

$$\begin{aligned}
E_{eff} &= 2EJ^2/(E^2 - J^2),\\
J_{eff} &= 2J^3/(E^2 - J^2).
\end{aligned} \tag{10}$$

Performing such decimation on all cells, we obtain an effective chain with all on-site energies E_{eff} and alternate hopping amplitudes, being J_{eff} for connecting sites originated from the same cell and J between neighboring cells. The dispersion relation of an infinite chain with alternate hopping amplitudes can be given by

$$E = E_{eff} \pm \sqrt{J^2 + J_{eff}^2 + 2JJ_{eff}\cos k}, \tag{11}$$

for a typical wavenumber k, where eigenstates with non-vanishing amplitudes at the sites of the effective chain are assumed. Substituting Eq. (10) into the one above yields the dispersive bands

$$E(k) = \mu\sqrt{3 \pm 2\sqrt{2}\cos{(k/2)}}J, \tag{12}$$

with $\mu = \pm$. The band limits are thus at $\mu(1 \pm \sqrt{2})J$.

However, the original array also supports eigenstates with *null* amplitudes at the sites connecting distinct cells. For example, for every cell there is a pair of eigenstates with energies $E = \pm J$ of the form $|E_{CLS}^{\pm}\rangle = (|3\rangle \pm |5\rangle - |4\rangle \pm |6\rangle)/2$. These are the so-called compact localized states (states restricted to their cell) that compose the flat bands at $E = \pm J$. We thus end up with a L-fold degeneracy at each of those levels, where L is the total number of cells. The total density of states per site of the entire channel can then be written as

$$DOS(E) = [\frac{1}{\pi}|dk/dE| + \delta(E - J) + \delta(E + J)]/6, \tag{13}$$

where $k(E)$ is taken from Eq. (11) and the degeneracies are taken into account.

In Fig. 2, we plot the analytical DOS of the pure channel alongside the disordered one obtained via exact numerical diagonalization for $N = 600$ ($L = 100$). The singularities exhibited in the pure graphene array are softened up by disorder. This is told by the development of tails in the band edges as well as by the replacement of the delta singularities by peaks with finite widths. The later is due to the degeneracy lifting of the compact localized modes within the hexagonal cells, with the width of the resulting peaks being proportional to the disorder strength. We will see shortly that the two ranges of allowed energies within the graphene array corresponds to the energy bands on which QST can be carried out.

In order to take a look into the localization properties of the channel, in Fig. 3 we plot the participation number defined as $P(E_k) = \sum_i |v_{i,k}|^2 / \sum_i |a_{i,k}|^4$. It basically covers the amount of sites having a significant overlap with mode k. For the eigenstates reminiscent from

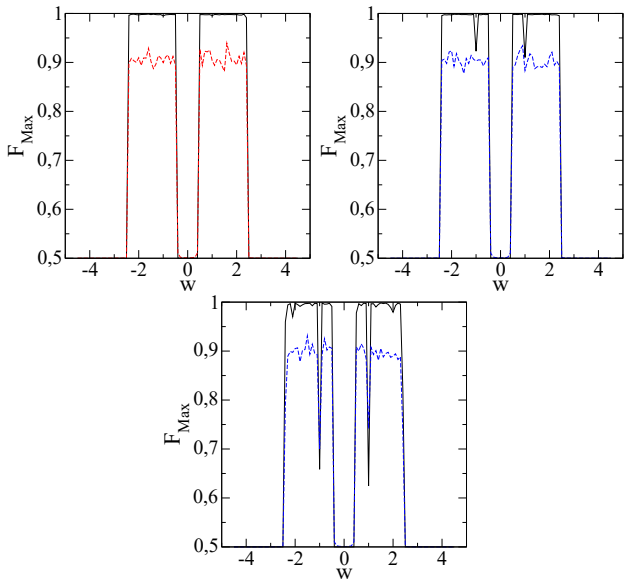

FIG. 4. Fidelity F_{Max} versus local sender and receiver energies w for $N = 600$ ($L = 100$ hexagonal cells) and (a) $b = 0$, (b) $b = 0.001J$, and (c) $b = 0.01J$. Solid (dashed) curves are for $g = 0.01J$ ($g = 0.1J$)

the effective alternate chain, the participation number remains relatively large and of the order of the chain size for the considered degree of disorder. This behavior is essential to the QST performance due to the presence of states of extended nature [41]. On the other hand, the levels $E = \pm J$ feature strongly localized modes which are restricted to each cell. As such, the QST protocol should become very sensitive to disorder when occurring at those levels (as controlled by w).

B. Qubit transfer

We shall now evaluate the dynamics of the single-qubit transfer through the channel in the weak-coupling regime $g \ll J$. Our numerical procedure is carried out via exact diagonalization of the single-excitation Hamiltonian [Eq. 4] that involves the whole $(N+2)\times(N+2)$ matrix. Basically, in order to compute the input-averaged fidelity F [3] we need to keep track of the transfer amplitude $f_{N+2}(t) = |\langle N+2|e^{-iHt}|1\rangle|$. Due to disorder, each sample dynamics features a different timescale. So, in order to evaluate the figure of merit of the protocol, we record the maximum value of the fidelity F_{Max} for $tJ \in [0, 10^6]$. This is enough time to guarantee a few end-to-end Rabi cycles given the transfer time $\tau \sim O(g^{-2})$ and we the set $g = 0.01J$ as the minimum coupling strength. In each simulation bellow we take the average of the maximum fidelity over 50 independent realizations of disorder.

We start by evaluating the protocol in the absence of disorder, ($b = 0$). The results are seen in Fig. 4(a), where F_{Max} is plotted as a function of the local sender and receiver energies w for different values of N and g.

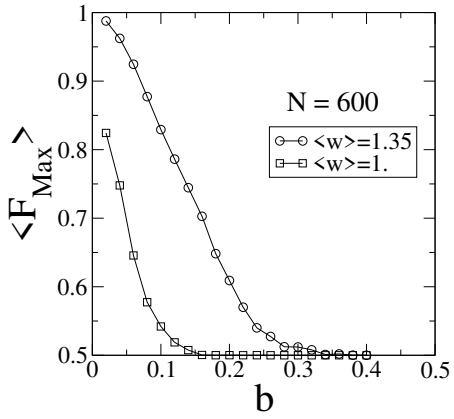

FIG. 5. F_{Max} versus the hopping disorder strength b for $N = 600$ and $g = 0.01J$ averaged over local energy levels surrounding $w = J$ and $w = 1.35J$ (about 50 levels). Again, the overall fidelity is further averaged over 50 independent disorder samples.

Therein we see that QST occur with high fidelity for a wide interval of energies w, specially for lower g, as expected, given that this is the primary condition for holding the two-level approximation [Eq. (5)]. The two energy bands on which the QST protocol runs is directly associated with the structure of the density of states of the hexagonal lattice as discussed previously.

We must take care, however, when making assumptions about the seemingly lack of QST for w set in the vicinity of the band center. For $b = 0$, note that $w = 0$ renders a proper effective resonant two-level (Rabi) dynamics as $h_s = h_r$ [see Eq. (6)] due to the particle-hole symmetry. The effective coupling [Eq. (7)], however, reads $J_{eff} = 2^{-L}g^2$ resulting in a transfer time that scales as $\tau \propto 2^L$. For the number of cells being considered in Fig. 4 ($L = 100$), τ is extremely large and thus unpractical.

We now turn our attention to the QST protocol in the presence of the hopping disorder as seen in Figs. 4(b) and 4(c). The performance remains nearly unaffected by the small amounts of disorder considered except when w gets in close resonance with the flat band levels $w = \pm J$. As we discussed in the previous section, that happens due to the residual presence of the compact localized states. When $b = 0$ they do not get involved in the QST because the sender and receiver are coupled to sites topologically protected from them. The smallest perturbation is then capable of lifting the degeneracy and mix $|E^{\pm}_{CLS}\rangle$ with the modes belonging to the dispersive bands. This is immediately felt in the perturbative Rabi regime given $w = \pm J$.

Finally, in order to get a broad picture of the QST performance against disorder in Fig. 5 we plot F_{Max} for a wider range of b, this time with the local energies set at $w = J$ and nearby for comparison. That clearly illustrates the higher sensitivity against disorder displayed by the flat band level. As long as w is tuned away from it, it

is possible to obtain a good QST fidelity on a reasonable amount of disorder $b \sim 0.1J$.

IV. CONCLUSIONS

We studied a QST protocol between two distant nodes of XY isotropic hexagonal spin-1/2 lattice subjected to off-diagonal (exchange interaction) disorder. By setting their coupling very weakly in comparison to the typical interaction strength scale within the channel, we showed it is possible to obtain high-fidelity QST up to a certain disorder threshold depending on the resonance conditions between the sender/receiver and the channel. There are two very unstable levels ($E = \pm J$) that lead to a rapid fidelity decay as we increase the disorder strength. This is reminiscent of the flat-band structure hosting compact localized states in the absence of disorder. To explain such a behavior we derived an effective model that describes a chain with alternate couplings, which is known to induce a topological gap and has been explored in the context of QST and quantum teleportation protocols [42–44].

Our work contributes to the design of solid-state devices for quantum communication in the presence of static noise and opens up venues for investigation of QST protocols in other geometries other than 1D channels, especially in flat-band lattices.

ACKNOWLEDGMENTS

This work was supported by CNPq, CAPES, FINEP, CNPq-Rede Nanobioestruturas, and FAPEAL (Alagoas State Agency).

[1] D. Castelvecchi, Ibm's quantum cloud computer goes commercial, Nature News **543**, 159 (2017).
[2] F. Arute *et al.*, Quantum supremacy using a programmable superconducting processor, Nature **574**, 505 (2019).
[3] J. Preskill, Quantum Computing in the NISQ era and beyond, Quantum **2**, 79 (2018).
[4] H. J. Kimble, The quantum internet, Nature **453**, 1023 (2008).
[5] S. Bose, Quantum communication through an unmodulated spin chain, Phys. Rev. Lett. **91**, 207901 (2003).
[6] M. Christandl, N. Datta, A. Ekert, and A. J. Landahl, Perfect state transfer in quantum spin networks, Phys. Rev. Lett. **92**, 187902 (2004).
[7] M. B. Plenio, J. Hartley, and J. Eisert, Dynamics and manipulation of entanglement in coupled harmonic systems with many degrees of freedom, New Journal of Physics **6**, 36 (2004).
[8] G. M. Nikolopoulos, D. Petrosyan, and P. Lambropoulos, Coherent electron wavepacket propagation and entanglement in array of coupled quantum dots, Europhys. Lett. **65**, 297 (2004).
[9] T. J. Osborne and N. Linden, Propagation of quantum information through a spin system, Phys. Rev. A **69**, 052315 (2004).
[10] A. Wójcik, T. Łuczak, P. Kurzyński, A. Grudka, T. Gdala, and M. Bednarska, Unmodulated spin chains as universal quantum wires, Phys. Rev. A **72**, 034303 (2005).
[11] A. Wójcik, T. Łuczak, P. Kurzyński, A. Grudka, T. Gdala, and M. Bednarska, Multiuser quantum communication networks, Phys. Rev. A **75**, 022330 (2007).
[12] Y. Li, T. Shi, B. Chen, Z. Song, and C.-P. Sun, Quantum-state transmission via a spin ladder as a robust data bus, Phys. Rev. A **71**, 022301 (2005).
[13] M. X. Huo, Y. Li, Z. Song, and C. P. Sun, The peierls distorted chain as a quantum data bus for quantum state transfer, Europhysics Letters **84**, 30004 (2008).
[14] J. Liu, G.-F. Zhang, and Z.-Y. Chen, Quantum state transfer via a two-qubit heisenberg xxz spin model, Physics Letters A **372**, 2830 (2008).
[15] G. Gualdi, V. Kostak, I. Marzoli, and P. Tombesi, Perfect state transfer in long-range interacting spin chains, Phys. Rev. A **78**, 022325 (2008).
[16] Z.-M. Wang, M. Byrd, B. Shao, and J. Zou, Quantum communication through anisotropic heisenberg xy spin chains, Physics Letters A **373**, 636 (2009).
[17] L. Banchi, T. J. G. Apollaro, A. Cuccoli, R. Vaia, and P. Verrucchi, Optimal dynamics for quantum-state and entanglement transfer through homogeneous quantum systems, Phys. Rev. A **82**, 052321 (2010).
[18] L. Banchi, T. J. G. Apollaro, A. Cuccoli, R. Vaia, and P. Verrucchi, Long quantum channels for high-quality entanglement transfer, New Journal of Physics **13**, 123006 (2011).
[19] T. J. G. Apollaro, L. Banchi, A. Cuccoli, R. Vaia, and P. Verrucchi, 99%-fidelity ballistic quantum-state transfer through long uniform channels, Phys. Rev. A **85**, 052319 (2012).
[20] S. Lorenzo, T. J. G. Apollaro, A. Sindona, and F. Plastina, Quantum-state transfer via resonant tunneling through local-field-induced barriers, Phys. Rev. A **87**, 042313 (2013).
[21] S. Paganelli, S. Lorenzo, T. J. G. Apollaro, F. Plastina, and G. L. Giorgi, Routing quantum information in spin chains, Phys. Rev. A **87**, 062309 (2013).
[22] S. Lorenzo, T. J. G. Apollaro, S. Paganelli, G. M. Palma, and F. Plastina, Transfer of arbitrary two-qubit states via a spin chain, Phys. Rev. A **91**, 042321 (2015).
[23] G. M. A. Almeida, F. Ciccarello, T. J. G. Apollaro, and A. M. C. Souza, Quantum-state transfer in staggered coupled-cavity arrays, Phys. Rev. A **93**, 032310 (2016).
[24] T. J. G. Apollaro, G. M. A. Almeida, S. Lorenzo, A. Ferraro, and S. Paganelli, Spin chains for two-qubit teleportation, Phys. Rev. A **100**, 052308 (2019).
[25] A. Kay, Perfect, efficient, state transfer and its application as a constructive tool, Int. J. Quantum Inform. **08**, 641 (2010).
[26] T. J. G. Apollaro, S. Lorenzo, and F. Plastina, Transport of quantum correlations across a spin chain, Int. J. Mod.

Phys. B **27**, 1345035 (2013).
[27] G. De Chiara, D. Rossini, S. Montangero, and R. Fazio, From perfect to fractal transmission in spin chains, Phys. Rev. A **72**, 012323 (2005).
[28] A. Zwick, G. A. Álvarez, J. Stolze, and O. Osenda, Spin chains for robust state transfer: Modified boundary couplings versus completely engineered chains, Phys. Rev. A **85**, 012318 (2012).
[29] M. Bruderer, K. Franke, S. Ragg, W. Belzig, and D. Obreschkow, Exploiting boundary states of imperfect spin chains for high-fidelity state transfer, Phys. Rev. A **85**, 022312 (2012).
[30] S. Ashhab, Quantum state transfer in a disordered one-dimensional lattice, Phys. Rev. A **92**, 062305 (2015).
[31] A. Kay, Quantum error correction for state transfer in noisy spin chains, Phys. Rev. A **93**, 042320 (2016).
[32] G. M. A. Almeida, C. V. C. Mendes, M. L. Lyra, and F. A. B. F. de Moura, Localization properties and high-fidelity state transfer in hopping models with correlated disorder, Annals of Physics **398**, 180 (2018).
[33] P. R. S. Junior, G. M. A. Almeida, M. L. Lyra, and F. A. B. F. de Moura, Quantum communication through chains with diluted disorder, Physics Letters A **383**, 1845 (2019).
[34] D. Messias, C. V. C. Mendes, G. M. A. Almeida, M. L. Lyra, and F. A. B. F. de Moura, Rabi-like quantum communication in an aperiodic spin-1/2 chain, Journal of Magnetism and Magnetic Materials **505**, 166730 (2020).
[35] G. M. A. Almeida, F. A. B. F. de Moura, and M. L. Lyra, Entanglement generation between distant parties via disordered spin chains, Quantum Information Processing **18**, 41 (2019).
[36] T. Haddad, S. Pinho, and S. Salinas, Critical behavior of ferromagnetic spin models with aperiodic exchange interactions, Brazilian Journal of Physics **30**, 4 (2000).
[37] T. Haddad and S. Salinas, Critical behavior of spin and polymer models with aperiodic interactions, Physica A: Statistical Mechanics and its Applications **306**, 98 (2002).
[38] R. Khomeriki and S. Flach, Landau-zener bloch oscillations with perturbed flat bands, Phys. Rev. Lett. **116**, 245301 (2016).
[39] N. Roy, A. Ramachandran, and A. Sharma, Interplay of disorder and interactions in a flat-band supporting diamond chain, Phys. Rev. Research **2**, 043395 (2020).
[40] O. Derzhko, J. Richter, and M. Maksymenko, Strongly correlated flat-band systems: The route from heisenberg spins to hubbard electrons, International Journal of Modern Physics B **29**, 1530007 (2015).
[41] G. M. A. Almeida, F. A. B. F. de Moura, and M. L. Lyra, Quantum-state transfer through long-range correlated disordered channels, Physics Letters A **382**, 1335 (2018).
[42] S. M. Giampaolo and F. Illuminati, Long-distance entanglement and quantum teleportation in coupled-cavity arrays, Phys. Rev. A **80**, 050301 (2009).
[43] S. M. Giampaolo and F. Illuminati, Long-distance entanglement in many-body atomic and optical systems, New Journal of Physics **12**, 025019 (2010).
[44] G. M. A. Almeida, F. A. B. F. de Moura, T. J. G. Apollaro, and M. L. Lyra, Disorder-assisted distribution of entanglement in xy spin chains, Phys. Rev. A **96**, 032315 (2017).